1   **KDM5A/B promotes HIV-1 latency and KDM5 inhibitors promote HIV-1 lytic reactivation**

2

3   **Authors**

4   Tai-Wei Li[a], Dawei Zhou[a], Zhenyu Wu[a], Guillaume N. Fiches[a], Xu Wang[b], Youngmin Park[a], Wei

5   Jiang[c], Wen-Zhe Ho[b], Andrew D. Badley[d], Netty G. Santoso[a], Jun Qi[e], and Jian Zhu[a,f,*]

6

7   **Affiliations**

8   [a]Department of Pathology, The Ohio State University Wexner Medical Center, Columbus, OH
9   43210, USA

10   [b]Department of Pathology and Laboratory Medicine, Temple University Lewis Katz School of
11   Medicine, Philadelphia, PA 19140, USA.

12   [c]Department of Microbiology and Immunology, Medical University of South Carolina,
13   Charleston, Charleston, SC 29425, USA

14   [d]Division of Infectious Diseases, Mayo Clinic, Rochester, MN 55902, USA

15   [e]Dana-Farber Cancer Institute, Boston, MA 02215, USA

16   [f]Department of Microbial Infection and Immunity, The Ohio State University Wexner Medical
17   Center, Columbus, OH 43210, USA

18

19   *To whom correspondence should be addressed: Jian Zhu (Jian.Zhu@osumc.edu).

20

21

22

23   **Key words:** HIV-1; KDM5; latency; lytic reactivation; reservoir; eradication; demethylation;
24   JQKD82; AZD5582; CD4+ T cells; monocytes; microglia

25

26

27

28   **Abstract**

29   Combinational antiretroviral therapy (cART) effectively suppresses HIV-1 infection,

30   replication, and pathogenesis in HIV-1 patients. However, the patient's HIV-1 reservoir still cannot

31   be eliminated by current cART or other therapies. One putative HIV-1 eradication strategy is

32   "shock and kill", which reactivates HIV-1 in latently-infected cells and induces their cytopathic

33   effect or immune clearance to decrease the patients' reservoir size. KDM5A and KDM5B act as

34   the HIV-1 latency-promoting genes, decreasing the HIV-1 viral gene transcription and reactivation

35   in infected cells. Depletion of KDM5 A/B by siRNA knockdown (KD) increases H3K4

36   trimethylation (H3K4me3) in HIV-1 Tat-mediated transactivation. We also found that the KDM5-

37   specific inhibitor JQKD82 can increase H3K4me3 at the HIV-1 LTR region during HIV-1

38   reactivation and induce cytopathic effects. We applied the JQKD82 in combination with the non-

39   canonical NF-κB activator AZD5582, which synergistically induced HIV-1 reactivation and cell

40   apoptosis in HIV-1 infected cells. These results suggested that the KDM5 inhibition can be a

41   putative HIV-1 latency-reversing strategy for the HIV-1 "shock and kill" eradication therapy.

42

43

44

45

46

47

48

Introduction

Globally, over 36 million individuals are infected with human immunodeficiency virus type 1 (HIV-1), and currently, no approved medicine or therapy can eradicate latent HIV-1 proviruses in infected patients. HIV infection dramatically affects patients' immune systems and causes acquired immunodeficiency syndrome (AIDS). Although combination antiretroviral therapy (cART) can suppress viral load below the detection limit in patients' blood and halt disease progression, HIV-1 can still reactivate from latently infected cells in lymphoid tissue that maintain persistent infection in cART-treated patients. The promising shock-and-kill strategy of HIV-1 eradication therapy involves combining latency-reversing agents (LRAs) and cART to reactivate the latent HIV-1 in the infected reservoir cells without inducing global T cell activation. During HIV-1 reactivation, the infected cells would be eliminated by the viral cytopathic effect and the cellular immune response from the cytolytic T lymphocytes (CTL) or natural killer (NK) cells [1-4]. Unfortunately, most of the currently used LRAs, such as the histone deacetylase (HDAC) inhibitor vorinostat, can induce viral reactivation (as the shock step) but cannot decrease the HIV-1 latent reservoir size (as the kill step) in the clinical trial setting [2, 5, 6]. The possible reasons for this include that the HIV-1 reservoir cells, such as CD4$^+$ T cells or macrophages, are resistant to the killing from CTLs [7-9] or adapt to avoid being killed by NK cells [10, 11]. Furthermore, the latently infected T cells can evade CTL/NK cells in the germinal follicles of lymphoid tissue [12-15]. For the future shock-and-kill strategy, we will need to focus on the kill strategies to facilitate the cell death of reservoir cells. Additionally, the putative strategy should activate the CTL/NK immunosurveillance or induce correct cytokine/chemokine to increase the killing of HIV-1 infected cells to eliminate the reservoir in the lymphoid tissue [9, 16].

3

71 Our previous research involved the CRISPR-knockout screening on latently infected cell lines

72 to investigate novel genes that control HIV-1 latency and reactivation [17]. We found that potential

73 latency-promoting genes (LPG) mainly participate in epigenetic regulation and chromatin

74 modification/organization. Notably, the knockdown of certain histone demethylases targeting

75 H3K4 or H3K36 methylation can induce HIV-1 reactivation. Also, the pan-Jumonji histone

76 demethylase inhibitor JIB-04 [18-20] could induce HIV-1 reactivation in the infected T cells or

77 monocytes. These results suggested that H3K4 or H3K36 methylation can be critical to HIV-1

78 reactivation and viral gene expressions. We also found that MINA53, which acts as the H3K36

79 demethylase, can promote HIV-1 latency due to decreased H3K36 trimethylation and inhibit

80 transcription elongation during HIV-1 reactivation [21]. This research focused on other LPG

81 candidates, H3K4 demethylases regulating HIV-1 latency/activation. H3K4 trimethylation

82 (H3K4me3) is located mainly at the transcription start site (TSS) to associate with TAF3 in the

83 TFIID complex [22-25] to facilitate transcription initiation. Previous studies showed that the HIV-

84 1 long terminal repeat (LTR) promoter enriched H3K4me3 during HIV-1 Tat-mediated

85 transactivation for viral gene transcription [26-28]. However, the detailed regulatory mechanism

86 of H3K4me3 in HIV-1 LTR for viral gene expression remains unclear. We previously identified

87 one H3K4me3 demethylase, lysine demethylase 5A (KDM5A), as a putative HIV-1 LPG that may

88 decrease the H3K4me3 level of HIV-1 LTR to suppress HIV-1 reactivation. We hypothesize that

89 if we can deplete KDM5A function through gene knockdown or pharmacology inhibition in HIV-

90 1 latent infected cells, we can trigger HIV-1 reactivation in infected cells, which can be killed by

91 the induced cytopathic effect or the CTL/NK cell immunosurveillance in the patient's tissue.

92 KDM5A is one of the KDM5 demethylases (KDM5 A, B, C, and D), which catalyzes

93 demethylation from H3K4me3 to H3K4me2 and then to the final product H3K4me1 [29-32].

94   Previously reported showed that KDM5A can induce PD-L1 expression [33, 34] that may suppress

95   the immune response for immune escape during HIV-1 infection [35-39]. The other KDM5,

96   KDM5B, has been identified to suppress immune sensing from the STING-GAS signaling [40]

97   and RIG-I signaling [41] to decrease innate immunity and antiviral responses. Furthermore,

98   KDM5B can prevent macrophages from releasing inflammatory cytokines like IL12 or TNF-α

99   during *L. donovani* infection [42]. We hypothesize that KDM5A or KDM5B depletion in HIV-1

100   latently infected cells induces HIV-1 reactivation and stimulates innate immunity to antiviral

101   responses. Furthermore, the H3K4m3 level of proapoptotic genes is usually low to prevent

102   accidental cell death during the native state [23], and thus, KDM5A depletion can promote cell

103   apoptosis [43, 44]. Therefore, we expect that inhibition of KDM5A or KDM5B can increase the

104   antiviral responses and proapoptotic genes with HIV-1 reactivation in latently infected cells to

105   eliminate the reservoir by HIV-1 induced cytopathic effects or antiviral-mediated programmed cell

106   death. Above all, this study focuses on the putative KDM5 depletion treatment to achieve the

107   shock-and-kill strategy for future putative HIV-1 eradication therapy.

108

109   **Results**

110   **Knockdown of KDM5A increases the HIV-1 Tat/LTR-driven transcription.**

111   To identify whether KDM5A depletion increases HIV-1 LTR transcription, we performed

112   KDM5A knockdown (KD) by siRNA in TZM-bl cells, which contain the HIV-1 LTR-driven

113   luciferase reporter [45-47]. First, we used immunoblotting (IB) to identify decreased KDM5A

114   expression with two specific siRNAs for knockdown (**Fig 1A**). Both KDM5A siRNAs decreased

115   KDM5A expression in transfected TZM-bl while increasing the H3K4me3 level and IRF3

116   phosphorylation. Previous studies also suggested that depletion of the KDM5 family (specifically,

117   KDM5B) can increase the IRF3 phosphorylation and transactivation to induce Type I interferon

118   and ISG expression for antiviral responses [40, 41, 48], which can promote cell apoptosis of HIV-

119   1 infected cells [49-52]. Also, the phosphorylated IRF3 can associate caspase-8 with Bax,

120   promoting the proapoptotic state for cell death [53]. We used the luciferase reporter assay to

121   identify whether the KDM5A KD affects HIV-1 LTR-driven transcription with or without HIV-1

122   Tat mediation (**Fig 1B**). We found that KD of siKDM5A#1 increases HIV-1 LTR transcription in

123   the native state of TZM-bl cells. Furthermore, the KD from two different siKDM5A increased

124   HIV-1 Tat-mediated LTR transcription in transfected TZM-bl cells. We also found that KDM5B

125   KD increases the H3K4me3 level, phosphorylation of IRF3 (**Fig 1C**), and HIV-1 Tat-mediated

126   LTR transcription (**Fig 1D**), consistent with the results of KDM5A KD in transfected TZM-bl

127   cells. These results suggested that decreasing the KDM5 family, such as KDM5A or KDM5B, can

128   increase HIV-1 reactivation and induce the IRF3-mediated proapoptotic state.

129   **KDM5 inhibitor JQKD82 increases HIV-1 reactivation and cell death in latently infected**

130   **cells.**

131   Since we showed that KDM5A and KDM5B KD both can promote HIV-1 LTR/Tat-mediated

132   transcription in TZM-bl cells, we went further to investigate whether the inhibition of all KDM5

133   family members (such as KDM5 A, B, C, and D) [30] can promote HIV-1 reactivation in latently

134   infected cells. We used the KDM5 inhibitor JQKD82 [44] to treat the CA5 cell line, the T

135   lymphocyte cell line integrated with the full-length HIV-1 proviral genome and the HIV-1 LTR-

136   driven GFP reporter [54, 55]. JQKD82 is the prodrug of KDM5-C49 [56] with the ester

137   metabolized group to inhibit KDM5 demethylase activity with high cellular permeability. We

138   treated the CA5 cells with a low concentration (10 or 25 µM) for 5 days to change the landscape

139   of histone methylation and epigenetic regulation for HIV-1 reactivation. The JQKD82-treated CA5

140   cells showed a significant increase in the GFP expression from HIV-1 reactivation compared to

141   the DMSO solvent control group (**Fig 2A-B**). These results showed that inhibiting KDM5

142   demethylase activity can directly induce HIV-1 reactivation in latently infected cells. To identify

143   whether KDM5 inhibitor JQKD82 can increase the cell death of HIV-1 infected cells, we treated

144   CA5 cells with JQKD82 for 5 days and stained them with LIVE/DEAD far-red dye to quantify the

145   cell death from the drug effect or HIV-1-induced cytopathic effect [57]. CA5 cells treated with 25

146   µM JQKD82 had higher rates of cell death than untreated CA5 cells or Jurkat parental cells with

147   the same treatment (**Fig 2C**). The results suggested that the inhibition of KDM5 can decrease cell

148   survival and increase cytopathic effects in HIV-1 latently infected cells.

149   We used the chromatin immunoprecipitation (ChIP) qPCR assay to identify whether

150   JQKD82 can increase the H3K4me3 level in the HIV-1 LTR to increase HIV-1 gene transcription

151   for reactivation [26]. We treated CA5 cells for 5 days with DMSO or 25 µM JQKD82 and then

152   harvested HIV-1 LTR-associated nucleosomes from cell lysates by the pull-down of anti-KDM5A

153   or anti-H3K4me3 antibodies. We extracted the nucleosome-associated DNA and performed qPCR

154   with the specific primers targeting the nucleosome binding sites in HIV-1 LTR (Nuc-0 and Nuc-

155   1) [17, 58, 59]. The results showed that JQKD82 increases the H3K4me3 level in Nuc-0 and Nuc-

156   1 (**Fig 2D**) at the HIV-1 LTR in CA5 cells compared to the untreated control group. The increase

157   of H3K4me3 in HIV-1 LTR, especially at the Nuc-1 site where the TSS of HIV-1 viral genes [23,

158   24], can promote the transcription initiation to increase HIV-1 viral gene expressions and

159   reactivation in the latently infected cells.

160   Also, we treated CA5 cells with a high dose of JQKD82 (50 or 100 µM) in a short period (48h),

161   which also promoted a significant increase in HIV-1 reactivation (**Fig S1 A-B**). The high dose of

162 JQKD82 induced significantly higher cell death of CA5 than untreated CA5 cells and Jurkat

163 parental cells under the same treatment (**Fig S1C**). These results suggested that a high dose of

164 JQKD82 treatment can induce HIV-1 reactivation and cell death of latently infected cells in a short

165 period.

166 **JQKD82 in combination with AZD5582, increases HIV-1 reactivation and cell death in**

167 **latently infected cells**

168 Previous studies indicated that the non-canonical NF-κB activator AZD5582 (AZD) increases

169 HIV-1 reactivation in ex vivo patient samples, humanized mouse models, and SIV-infected

170 macaque models [60]. However, AZD5582 could not decrease the HIV-1 reservoir size in SIV-

171 infected macaques. We hypothesized that combining JQKD82 and AZD5582 boosts HIV-1

172 reaction and induces cell death for the shock-and-kill strategy for HIV-1 eradication therapy. We

173 treated CA5 cells with JQKD82 for 3 days and then refreshed the treatment with or without 0.2

174 μM AZD5582 for 2 days. Treated cells were harvested, and LIVE/DEAD staining was performed;

175 using FASC, the cells were then analyzed for HIV-1 reactivation from GFP expression and cell

176 death from APC dye signals (**Fig 3A**). AZD5582 induced ~20% GFP expression from the treated

177 CA5 cells, and JQKD82 further strengthened the AZD5582-mediated HIV-1 reactivation in the

178 treated CA5 cells (**Fig 3B**). Furthermore, JQKD82 significantly increased the cell death of

179 AZD5582-reactivated CA5 cells compared to the Jurkat cells with the same combination treatment

180 (**Fig 3C**). We used an IB assay to identify the protein markers for cell responses from the

181 JQKD82/AZD5582-treated Jurkat and CA5 cells (**Fig 3D**). We found that JQKD82 increases the

182 total H3K4me3 level in both Jurkat and CA5 cells, and JQKD82 can directly increase the HIV-1

183 p55/p24 expression in the treated CA5 cells. With the JQKD82/AZD5582 combination treatment,

184 JQKD82 increased the HIV-1 p55/p24 expression and the PARP cleavage (as the apoptosis marker

185   [61, 62]) in the AZD5582-reactivated CA5 cells. We also applied a high dose of JQKD82

186   cotreatment with AZD5582 to Jurkat and CA5 cells for 48 hours (**Fig S2A**). The

187   JQKD82/AZD5582 cotreatment increased the HIV-1 reactivation significantly more than a single

188   JQKD82 or AZD5582 treatment (**Fig S2B**). The JQKD82/AZD5582 cotreatment also induced

189   higher cell death in CA5 cells than single-drug treated CA5 cells and the JQKD82/AZD cotreat-

190   Jurkat cells (**Fig S2C**). However, the JQKD82/AZD5582 cotreatment also caused high

191   cytotoxicity in Jurkat parental cells (~20% cell death).

192   We treated CA5 cells with another prodrug of KDM5-C49, KDM5-C70 [56], cotreated with

193   AZD5582 for 48h. The results suggested that the high concentration of KDM5-C70 can induce

194   HIV-1 reactivation in CA5 cells (**Fig S3A-B**). Also, KDM5-C70 synergistically increased

195   AZD5582-induced HIV-1 reactivation in CA5 cells. However, KDM5-C70 did not significantly

196   increase the cell-killing effect in CA5 cells with or without AZD5582 treatment (**Fig S3C**)

197   compared to JQKD82, which has better cell permeability than KDM5-C70 [44].

198   We performed the DHIV-1 infected primary Tcm model with JQKD82/AZD5582 combination

199   treatment. We identified that the JQK82 and JQKD82/AZD5582 treatment could increase the

200   cellular HIV-1 Gag mRNA level in the primary HIV-1 infected Tcm cells compared to the DMSO

201   control group (**Fig 4A**). We also treated the s peripheral blood mononuclear cells (PBMCs with

202   CD8$^+$ T cell depletion) from HIV-1 aviremic patients with the JQKD82/AZD5582 combination

203   treatment and harvested the cultured supernatant to detect HIV-1 viral RNA release. The results

204   showed that the JQKD82/AZD5582 combination treatment increased HIV-1 viral RNA release

205   from infected PBMCs in 4 donors (**Fig 4B**), suggesting that JQKD82/AZD5582 can induce HIV-

206   1 reactivation in HIV-1 aviremic patient' PBMCs. In conclusion, JQKD82 can strengthen

207   AZD5582-mediated HIV-1 reactivation and cell killing in HIV-1 latent infected cells. A low dose

9

208 of JQKD82, combined with AZD5582, can be a gradual HIV-1 eradication therapy for decreasing

209 the latently infected cell population and HIV-1 reservoir.

210 **Inhibition of KDM5 A/B increases HIV-1 LTR/Tat-mediated transcription in other types of**
211 **cells.**

212 We identified that the inhibition of KDM5 increases HIV-1 reactivation in latently infected

213 CD4$^+$ T cells, and we investigated whether the KDM5s regulate the HIV-1 reactivation in the

214 monocyte/macrophage reservoirs. We used HC69 microglia cells containing HIV-1 LTR/Tat-

215 driven GFP reporter, mimicking the cell behavior of the HIV-1 latency reservoir in the central

216 nerve system (CNS) [63-65]. We treated HC69 cells with a KDM5 inhibitor, JQKD82, for 5 days

217 and found that JQKD82 significantly increased HIV-1 LTR/Tat-driven GFP expression (**Fig 5A-**

218 **B**), but JQKD82 did not significantly increase the cell death of HC69 cells (**Fig 5C**). We also used

219 siRNA KD of KDM5A or KDM5B to identify whether H3K4me3 demethylase promotes HIV-1

220 latency in infected microglia. The KD of KDM5A or KDM5B significantly increased HIV-1

221 LTR/Tat-driven GFP in transfected HC69 cells (**Fig 5 D-E**) but did not cause significant cell death

222 in microglia cells (**Fig 5F**). These results suggested that inhibition of KDM5A or KDM5B can

223 increase HIV-1 reactivation in the monocyte/macrophage reservoir and need to be combined with

224 other reagents or interventions to eradicate HIV-1 infected microglia cells in CNS.

225 We also gave JQKD82/AZD5582 combination treatment to U1/HIV cells, the monocytic cell

226 line latently infected by HIV-1 [66-68], for 5 days (**Fig S4A**). The results showed that

227 JQKD82/AZD5582 combination treatment significantly increases HIV-1 Gag protein expression

228 (**Fig S4B)** and mRNA level (**Fig S4C**). These results suggested that JQKD82/AZD5582

229 combination treatment induces HIV-1 reactivation in latently infected monocytes.

230

Discussion

231

232   The results of this study suggested that the depletion of KDM5A or KDM5B can raise HIV-1

233   Tat/LTR mediated transcription to promote HIV-1 reactivation (**Fig 1**). We hypothesized that

234   KDM5s (Specially KDM5A) can recognize the H3K4me3 at HIV-1 LTR and catalyze the H3K4

235   demethylation to increase the threshold for reactivation and promote latency in HIV-1 infected

236   cells. After KDM5 depletion increases in the H3K4me3 level at HIV-1 LTR sites, H3K4me3

237   facilitates the transcription initiation and HIV-1 Tat/TAR-mediated reactivation. We also found

238   that the KD of KDM5A/B is insufficient to turn on HIV-1 LTR transcription in TZM-bl cells

239   directly. However, KDM5-inhibitor treatment may increase other viral protein expressions, such

240   as HIV-1 Tat, as positive feedback to facilitate the HIV-1 reactivation in the HIV-1 latent CA5

241   cells (**Fig 2**). In conclusion, the axis of KDM5/H3K4me3/Tat interaction to regulate the

242   transactivation of HIV-1 LTR promoter can be critical for the epigenetic controls of HIV-1

243   reactivation and latency in latently infected cells.

244   In previous studies about the epigenetic control of HIV-1 reactivation, HDAC inhibitors such

245   as valproic acid [69, 70], panobinostat, or SAHA (Vorinostat) [71-73] were used, which could

246   induce HIV-1 reactivation in the latently infected cell line, primary infected cell model, or even in

247   ex vivo aviremic ART-treated patients' infected cells. However, these HDAC inhibitors could not

248   pass human clinical as they were being insufficient to progressively reactivate HIV-1 latent

249   infected cells in the lymphoid tissue over a long period [5, 74], failing to terminate HIV-1 infection

250   in resting T cells during HIV-1 reservoir expansion [75, 76], or limiting the cell killing effect [6,

251   77-80] to decrease the reservoir in the patient's body [81]. The future shock-and-kill therapy would

252   need to pursue or combine the different putative drugs to enhance reactivation and promote the

253   killing of HIV-1 reservoirs. Previous studies suggested that KDM5A and KDM5B can associate

11

254 with HDAC-complex to perform epigenetic silencing cooperatively [82-85]. KDM5 inhibitors

255 combined with HDAC inhibitors could benefit future HIV-1 eradication by improving the

256 reactivation and cell-killing effects. Also, the depletion of KDM5B can potentially increase

257 antiviral immunity and promote IRF3 signaling (**Fig 1C**), which can increase the IRF3-mediated

258 or antiviral-induced cell death [53, 86-88] to decrease the HIV-1 reservoir expansion and archive

259 the shock-and-kill therapeutic process.

260 JQKD82 is the prodrug with the ester-modified group of the functional metabolite KDM5-

261 C49, which can block the α-ketoglutarate catalytic site in the KDM5 Jumonji-C domain [44, 56].

262 In a previous study, JQKD82 showed better cell permeability and cellular accumulation than other

263 C49-derivatives or prodrugs and significantly increased the global H3K4me3 level in treated cells.

264 In RNA-Seq analysis, the gene expressions after JQKD82-treatment increased in Type I interferon

265 and inflammatory responses [44]. Like other KDM5 inhibitors and depletions, JQKD82 can cause

266 the shut-down cell cycle and promote the proapoptotic state and innate immunity responses [43,

267 44, 89, 90]. We applied the low doses of JQKD82 treatment (below 25 μM) for an extended period

268 (at least 5 days) to HIV-1 latent cells and induced HIV-1 reactivation and their cell death (**Fig 2**).

269 We also applied the high doses of JQKD82 treatment (beyond 50 μM) to latently infected cells

270 and uninfected parental cells for a short time (48h). This treatment induced HIV-1 reactivation but

271 also caused high cell-killing effects in uninfected parental cells (**Fig S1C**). These results suggested

272 that intense JQKD82 can cause high cytotoxicity in uninfected cells.

273 In this study, we used the KDM5 inhibitor, JQKD82, in combination with the non-canonical

274 NF-κB activator, AZD5582, to synergistically increase HIV-1 reactivation and cell death in

275 latently infected cells. AZD5582 is a SMAC-mimetic analog that causes inhibitor of apoptosis

276 proteins (IAPs) self-ubiquitination and degradation [60, 91] to increase p52-RelB nuclear

277   translocation and turn on downstream gene expressions [92]. AZD5582 and other SMAC-mimetic

278   IAP inhibitors can also increase the cellular proapoptotic state for induced HIV-1 cytopathic killing

279   [93-96]. AZD5582 could reactivate HIV-1/SIV in patient cell samples and animal models [60].

280   However, AZD5582 alone could not decrease the reservoir size in SIV-infected macaques and

281   increase antiviral immunity responses. Our results showed that the combination of JQKD82 and

282   AZD5582 treatment boosted the HIV-1 reactivation and induced apoptosis (**Fig 3**) in the latently

283   infected cells and did not cause severe cytotoxicity in the uninfected parental cells. We also found

284   that another KDM5-C49 prodrug, KDM5-C70, can synergetically increase AZD5582-induced

285   HIV-1 reactivation, but KDM5-C70 cannot increase the cell-killing effect as JQKD82 treatment

286   (**Fig S3**). These results suggested that JQKD82 has a better cell permeability and KDM5-inhibitory

287   effect [44], promoting a higher proapoptotic state in HIV-1 latently infected CD4$^+$ T cells and

288   monocytes. We also performed JQKD82/AZD5582 combination treatment to the HIV-1 patient's

289   PBMCs (with the depletion of CD8$^+$ T cells) and found that JQKD82/AZD5582 can induce HIV-

290   1 reactivation and increase the release of HIV-1 viral RNA from 4 donors' infected PBMC (**Fig**

291   **4B**). In the future, we will test more PBMC samples from different HIV-1 patients to confirm these

292   preclinical results. Also, we will quantify the change in reservoir sizes of JQKD82/AZD5582-

293   treated HIV-1 infected PBMCs by the quantitative viral outgrowth assay (QVOA) to validate

294   whether the JQKD82/AZD5582 combination treatment can be the candidate for shock-and-kill

295   therapy.

296   HIV-1 infected microglia cells are the latency reservoir and cause the abnormal inflammatory

297   state for the pathogenesis of HIV-1-associated neurocognitive disorder (HAND), even under the

298   cART control [97]. In order to understand the HIV-1 reactivation mechanism of microglia and

299   develop a therapy targeting HIV-1 reservoirs in the CNS, we used the immortalizing human

300　primary microglia with HIV-1 LTR/Tat-mediated GFP reporter, HC69 cell line [63-65] to

301　investigate whether the KDM5 depletion can increase HIV-1 reactivation and cytopathic effect.

302　The JQKD82 treatment and KDM5 A/B siRNA KD can increase the HIV-1 LTR/Tat

303　transactivation in HC69 microglia (**Fig 3.5**). However, the depletion of KDM5, whether by

304　pharmaceutical inhibitors or siRNA knockdown, can not increase the cytopathic effect or cell death

305　in HC69 microglia. HC69 cells contain the HIV-1 LTR/Tat driven GFP reporter, but HC69 cells

306　have the deletion of HIV-1 Gag, Pol, and other accessory viral proteins, which cause single-round

307　infection without generating severe cytopathic effects during HIV-1 reactivation. These results

308　suggested that the KDM5 inhibitors can be a putative LRA for the HIV-1 reactivation in infected

309　microglia, but we need to identify their cell-killing effects in the different HIV-1 infected microglia

310　models.

311　　In this study, we demonstrated that the depletion of KDM5 A/B by siRNA KD or enzymatic

312　inhibitor JQKD82 increases the H3K4me3 at the HIV-1 LTR site and HIV-1 Tat-mediated viral

313　gene transcriptions for HIV-1 reactivation. The KDM5 depletion combination with non-canonical

314　NF-κB activator AZD5582 can significantly increase cell death in HIV-1 infected cells. The

315　JQKD82/AZD5582 combination treatment can promote the HIV-1 reactivation and proapoptotic

316　state to eliminate the HIV-1reservoir for putative HIV-1 cure therapy.

317

318　**Material and methods**

319　**Cell culture**

320　　TZM-bl, Jurkat, and U1 cell lines were obtained from the National Institutes of Health (NIH)

321　AIDS reagent program. The Jurkat-derived CA5 cell line latently infected with replication-

322   competent, full-length HIV-1 genome was provided by Dr. O. Kutsch [54, 55]. TZM-bl and

323   HEK293T (Cat. # CRL-3216, ATCC) cells were cultured in Dulbecco's modified Eagle's medium

324   (DMEM, Cat # D5796, Sigma). All T cell lines were cultured in Roswell Park Memorial Institute

325   (RPMI) 1640 medium (Cat # 11875093, Gibco). Completed cell culture medium contained 10%

326   fetal bovine serum (FBS, Cat. # 10437028, Thermo Fisher), penicillin (100 U/ml) /streptomycin

327   (100 μg/ml) (Cat. # MT30002CI, Corning). Primary peripheral blood mononuclear cells (PBMCs)

328   were maintained and cultured with a completed RPMI medium with 1× minimum essential

329   medium nonessential amino acid (Cat #11140-050, Gibco), 1× sodium pyruvate (Cat #11360-070,

330   Gibco), and 20 mM HEPES (Cat #15630-080, Gibco). Human recombinant IL-2 (rIL-2, Roche) at

331   30 U/ml was supplied to primary cells every 2 days [57]. HC69 and the parental C20 microglia

332   cells were cultured in BrainPhys medium (Cat. #05790, StemCell Technologies) containing N2

333   supplement (Cat. #17502048, Gibco), penicillin (100 U/ml) /streptomycin, 100 μg/mL normocin

334   (Cat. #ant-nr-1, InvivoGen), 25 mM glutamine (Cat. #25030081, Gibco), 1% FBS and 1 μM

335   DEXA (Cat. #D4902, Sigma) freshly added to the cell culture [63-65].

336   **Compounds, antibodies, and plasmid**

337   Recombinant human TNF-α (Cat. # 554618) was purchased from BD. Biosciences. KDM5

338   inhibitor JQKD82 was synthesized and generously gifted by Dr. Jun Qi's lab [44]. AZD-5582 (Cat.

339   # CT-A5582) was purchased from Chemie Tek. KDM5-C70 (M60192-10S) was purchased from

340   Xcess Biosciences.

341   Mouse anti-GAPDH antibody (Cat. # sc-32233) was purchased from Santa Cruz

342   Biotechnology. Rabbit anti-phosphorylated IRF3 antibody (Cat. # 4947S), rabbit anti-IRF3

343   antibody (Cat. # 4302S), rabbit anti-H3 antibody (Cat. # 9715S), rabbit anti-PARP antibody (Cat.

344 # 9542T), goat HRP-conjugated anti-mouse IgG antibody (Cat. # 7076S), and goat HRP-

345 conjugated anti-rabbit IgG antibody (Cat. # 7074) were purchased from Cell Signaling Technology.

346 Mouse anti-KDM5A antibody (Cat # 91211) and Mouse anti-H3K4me3 antibody (Cat #61379)

347 were purchased from Active Motif. HIV-1 Gag p24 IgG1 monoclonal antibody was produced from

348 the hybridoma cell line (NIH AIDS reagent program).

349 The pQC-HIV-1 Tat was constructed by subcloning C terminal Flag tag fused HIV-1 Tat into

350 the pQCXIP retroviral empty vector (Clontech) using NotI and BamHI sites [98].

Transient transfection

352 For KDM5A knockdown, 10 nM siRNA (siKDM5A; #1: siRNA ID: s11835: 5'-

353 CCGCUAAAGUGGAAGCUAUtt-3'; #2: siRNA ID: s11836: 5'-GCGAGUUUGUUGUGACA-

354 UUtt-3'; siKDM5B #1: siRNA ID: s21145: 5'-GGCAGUAAAGGAAAUCGAAtt ; #2: siRNA Id:

355 s21146: 5'-GGAAGAUCUUGGACUUAUUtt-3', Ambion by Life technologies; non-targeting

356 control: Silencer™ Negative Control No. 4 siRNA, si N.T., Cat. # AM4641, Invitrogen) was

357 reversely transfected in TZM-BL cells using Lipofectamine™ RNAiMAX Transfection Reagent

358 (Cat. # 13778030, Invitrogen). Cells were kept in culture for 48h and continued the further

359 experiment subjected to IB of KDM5A or KDM5B to evaluate the knockdown efficacy.

360 For HIV-1 Tat overexpression to induce the HIV-1 LTR-driven reporter assay, we performed

361 the transient transfection of pQC-HIV-1 Tat or pQCXIP empty vector control in TZM-BL cells

362 using Fugene6 transfection reagents (Cat. # E2691, Promega). Briefly, cells were seeded and

363 incubated with the mixture of plasmids with Fugene 6 for 24 h, following the manufacturer's

364 protocol. The medium was changed and further cultured for an additional 24h for harvesting and

365 performed following experiments.

Luciferase reporter assays

Treated TZM-BL cells were trypsinized and harvested for luciferase activity assay (One-Glo System, Cat. # E6110, Promega) following the manufacturer's protocol. Chemiluminescence was determined by using the was detected using Biotek Cytation5 and analyzed by GEN5 software (Biotek). In the HIV-1 LTR-driven reporter assay, the relative light unit (RLU) of luciferase luminescence was divided by the total protein input (RLU/µg) quantified by the BCA assay kit (Cat. #23225, Thermo Scientific). The readouts were normalized with the siNT/pQC-empty vector-transfected TZM-BL group.

Protein immunoblotting

Protein immunoblotting was performed following our previously published protocols [57, 99]. Briefly, cells were harvested, washed by PBS, and pelleted. Cell pellets were lysed in RIPA buffer (Cat. #20-188, Millipore) containing protease inhibitor cocktail (Cat. # A32965, Thermo Scientific) on ice, followed by brief sonication to prepare cell lysate. The BCA assay kit (Cat. #23225, Thermo Scientific) was used to quantify the total protein amount in cell lysate, which was boiled in the SDS loading buffer with 5% β-mercaptoethanol (Cat. #60-24-2, Acros Organics). The denatured protein samples were separated by Novex™ WedgeWell™ 4-20% SDS-PAGE Tris-Glycine gel and transferred to PVDF membrane (iBlot™ 2 Transfer Stacks, Invitrogen) using iBlot 2 Dry Blotting System (Cat. # IB21001, Thermo Scientific). The membranes were blocked by 5% milk in PBST and probed by the specific primary antibodies at 4°C overnight, followed by the HRP-conjugated secondary antibodies. The membranes were developed using the Clarity Max ECL substrate (Cat. # 1705062, Bio-Rad).

Cell viability assay

17

388   The death of HIV-1-reactivated or compound-treated cells was determined using the

389   LIVE/DEAD Fixable Far Red Dead Cell Stain Kit (Cat. # L10120, Invitrogen), following the

390   manufacturer's protocol [57]. In brief, the treated cells were washed and incubated with the

391   working dilution of LIVE/DEAD dye for 30 mins and then washed with PBS. Stained cells were

392   fixed with 4 % paraformaldehyde (Cat. # 15714S, Electron Microscopy Sciences), and analyzed

393   the APC signaling by the BD Accuri C6 Plus flow cytometer (BD Biosciences).

Flow cytometry

395   Cells were harvested, washed twice with PBS, fixed by 4% paraformaldehyde, and then

396   resuspended in 2% BSA with PBS for FASC analysis. The cell samples were analyzed using an

397   Accuri C6 Plus flow cytometer (BD Biosciences) with forward versus side scatter (FSC-A versus

398   SSC-A) gating and the corresponding optical filters for the excitation/emission of fluorescence

399   expression. The percentage of fluorescence-positive cells was determined by using the FlowJo

400   V10 software.

Chromatin immunoprecipitation (CHIP) assay

402   ChIP assay was conducted as described previously [17, 59, 99, 100]. Cells were cross-

403   linked by using 0.5% paraformaldehyde for 10 min, followed by treatment with 125 mM glycine

404   to quench the reaction for 5 min. After washing with cold PBS twice, cells were lysed for 10 min

405   on ice in CE buffer (10 mM HEPES-KOH, 60 mM KCl, 1 mM EDTA, 0.5% NP-40, 1 mM DTT,

406   pH: 7.9 with protease inhibitor cocktail). The nuclei were pelleted by centrifugation at $700 \times g$ for

407   10 min at 4°C and resuspended in SDS lysis buffer (1% SDS, 10 mM EDTA, 50 mM Tris-HCl,

408   Ph: 8.1 with protease inhibitor cocktail). Nuclear lysates were sonicated for 2 min to fragment

409   genomic DNA and subsequently diluted with ChIP dilution buffer (0.01% SDS, 1% Triton X-100,

18

410   1.2 mM EDTA, 16.7 mM Tris-HCl, 150 mM NaCl, pH: 8.1 with protease inhibitor cocktail). The

411   lysates were incubated overnight at 4°C with specific antibodies or control mouse IgG (Cat. # sc-

412   2025, Santa Cruz). Protein A/G beads (Cat. # 88803, Pierce) were pre-blocked with 0.5 mg/ml

413   BSA and 0.125 mg/ml herring sperm DNA (Cat. 15634-017, Invitrogen) for 1 h at room

414   temperature and then added to the lysate-antibody mixture for another incubation at 4°C for 2 h.

415   Beads were washed with the following buffers: low salt wash buffer (0.1% SDS, 1% Triton X-100,

416   2 mM EDTA, 20 mM Tris-HCl, 150 mM NaCl, pH 8.1); high-salt wash buffer (0.1% SDS, 1%

417   Triton X-100, 2 mM EDTA, 20 mM Tris-HCl, 500 mM NaCl, pH 8.1); LiCl buffer (0.25 M LiCl,

418   1% NP-40, 1% Na-deoxycholate, 1 mM EDTA, 10 mM Tris-HCl, pH 8.1); and TE buffer (10 mM

419   Tris-HCl, 0.1 mM EDTA, pH 8.1), and were eluted with fresh elution buffer (1% SDS, 0.1 M

420   NaHCO$_3$) at room temperature. The eluted samples were incubated at 65°C overnight in the

421   presence of 0.2 M NaCl to disassociate the cross-linking of protein/bound DNA. The eluted

422   samples were then treated with proteinase K (Cat. #EO0491, Thermo Fisher Scientific) for protein

423   digestion at 50°C for 2h, and the DNA species were precipitated by using UltraPure™

424   Phenol:Chloroform: Isoamyl Alcohol reagent (Cat. # 15593031, Thermo Fisher Scientific) with

425   the manufacturer's protocol. The DNA pellets were dried out and resuspended in water, and the

426   pull-down DNA was quantified by qPCR.

427   **Quantitative reverse transcription PCR (RT-qPCR and ChIP-qPCR**

428   RT-qPCR assays were performed following the previously published protocol [101]. Total

429   RNAs from harvested cells were extracted using the NucleoSpin RNA extraction kit (Cat. #

430   740955.250, MACHEREY-NAGEL), and ~1 μg RNA was reversely transcribed using the

431   iScript™ cDNA Synthesis Kit (Cat. # 1708890, Bio-Rad). Real-time qPCR was conducted using

432   the iTaq™ Universal SYBR® GreenSupermix (Cat. # 1727125, Bio-Rad). The PCR reaction was

433   performed on a Bio-Rad C.F.X. connect qPCR machine under the following conditions: 95 °C for

434   10 m, 50 cycles of 95 °C for 15 s, and 60 °C for 1 m. Relative gene expression was normalized to

435   GAPDH internal control as the $2^{-\Delta\Delta Ct}$ method: $2^{(\Delta CT\ of\ targeted\ gene\ -\ \Delta CT\ of\ GAPDH)}$. The qPCR primers

436   were used in this study as below: HIV-1 Gag (F: CTGAAGCGCGCACGGCAA; R: 5'-CTGAAG

437   CGCGCACGGCAA-3'), β actin (F: 5'-GGACCTGACTGACTACCTCAT-3'; R: 5'-

438   GTAGCACAGCTTCTCCTTAAT-3'), KDM5A (F: 5'-CAACGGAAAGGCACTCTCTC-3'; R:

439   5'-CAAGGCTTCTCGAGGTTTG-3'), KDM5B (F: 5'- ATTCTGTTGGCACATTGAAGACC-

440   3'; R: 5'- AGCATACCCTGGGACTCCATAC-3').

441   ChIP-qPCR assays were performed by the elute DNA from the ChIP assay. The fold

442   enrichment from ChIP was normalized to IgG pull-down control in the same treatment as the 2^{-}

443    $^{\Delta\Delta Ct}$ method: $2^{(\Delta CT\ of\ targeted\ gene\ -\ \Delta CT\ of\ IgG\ pull-down)}$. The PCR primers for the bound nucleosomes of

444   HIV-1 LTR were: Nuc-0 (F: 5'-GAAGGGCTAATTTGGTCCCA -3'; R: 5'-GATGCAGCTCTC

445   GGGCCATG-3'), Nuc-1 (F: 5'-AGTGTGTGCCCGTCTGT-3'; R: 5'-TTGGCGTACTCACCA

446   GTCGC-3').

DHIV-1 preparation

448   Envelope-deficient DHIV backbone plasmid was provided by Dr. Vicente Planelles [102].

449   VSV-G pseudo-typed DHIV viruses were prepared by transfecting HEK293T cells with DHIV

450   vector and pMD2.G-VSV-G plasmids with Turbofect reagent (Cat. #R0531, Thermos scientific)

451   following the manuscript protocol. The supernatant containing VSV-DHIV viral particles was

452   harvested at 48 hours after transfection. Supernatant-containing viruses were centrifuged to

453   remove cellular debris, filtrated with 0.45-μm membrane filters, and stored at −80°C [57]. Viral

454   supernatant was tittered by infecting Jurkat cells with serial dilution for 48h and performing anti-

455   HIV-1 Gag immunofluorescence staining. The percentages of HIV-1 Gag positive cells from

456   different dilutions of supernatant were analyzed by FASC. The infectivity of the VSV-G DHIV-1

457   supernatant ranged from $1.7\text{-}2.9 \times 10^7$ IU/ml.

458   **Establishment of HIV-1 latency in human primary CD4+ T cells**

459   A primary CD4+ Tcm cell model of HIV-1 latency established by Dr. Vicente Planelles'

460   group was used as previously described with modifications [57, 102]. The frozen Human primary

461   peripheral blood $CD4^+$ T cells (Cat. # 200-0165, Stemcell Technologies) were stimulated on a 96-

462   well Nunc-Immuno Maxi Sorp plate precoated with soluble anti-CD3/CD28 antibodies in RPMI

463   complete medium containing TGF-β1 (10 ng/ml), anti-human IL-12 (2 μg/ml), and anti-human IL-

464   4 (R&D Systems) (1 μg/ml) for 3 days. After 3-day activation, the naïve cells were considered

465   nonpolarized, differentiated into a TCM-like phenotype, and cultured in RPMI complete medium

466   with Human rIL-2 (30 U/ml). On day 7, the Tcm-like cells were infected with VSV-G pseudo-

467   typed DHIV (MOI: 1.0; p24 input 100 ng/ml) through spinoculation with 1×10^6 cells/ml with 8

468   μg/ml polybrene (Cat. # TR-1003-G, Sigma) at 1741g at 37°C for 2 hours. Infected Tcm cells were

469   cultured for 10-day incubation to establish HIV-1 latency. KDM5 inhibitor JQKD82 (10 μM) was

470   treated for DHIV-infected T cm for 3 day and refreshed with JQKD82-treatment with or without

471   0.1 μM AZD-5582. We harvested these cells for RNA extraction and RT-qPCR analysis for

472   detecting HIV-1 Gag mRNA level (β actin mRNA as the internal control).

473   **Ex vivo analysis using CD8-depleted PBMCs of aviremic patients**

474   Consented HIV-1 positive, cART-treated, aviremic patients (<20 copies per mL) were

475   recruited through the AIDS clinic at the Mayo Clinic to donate whole blood via leukapheresis.

476   Peripheral blood mononuclear cells (PBMCs) were then isolated and cultured in a complete

477   medium supplemented with 30 U/mL interleukin-2 (IL2) and in the presence of 600 nM of

478   Nevirapine (Cat. #, Sigma) for 3 days. PBMCs were subjected to $CD8^+$ T cells depletion by

479   negative selection using the CD8 MicroBeads (Cat. # 130-045-201, Miltenyi Biotec). $CD8^+$ T

480   cells-depleted PBMCs were treated with or without 10 μM JQKD82 for 3 days, and then the

481   JQKD82-untreated were refreshed in the cultured medium with no-treatment (mock), 0.1 μM

482   AZD5582 (AZD), or PMA (100 ng/ml) +ionomycin (0.5 μg/ml) or anti-CD3/CD28 Dynabeads

483   (ratio: 1 bead to 2 cells; Cat. # 11161D, Gibco). The JQKD82-treated cells were changed medium

484   with 10 μM JQKD82 with or without 0.1 μM AZD5582. Supernatants were collected and

485   subjected to the extraction of HIV viral RNAs by using the QIAmp® Viral RNA Kit (Cat. #52904,

486   Qiagen). The ultrasensitive nested qPCR assay was performed to quantify HIV viral RNA copies

487   as previously described [100, 103, 104]. HIV-1 IIIB RNAs were extracted by the NucleoSpin RNA

488   Virus kit (Cat. #740956.10, MACHEREY-NAGEL) and quantified with copy numbers by the

489   Lenti-X qRT-PCR titration kit (Cat. #631235, Takara Bio). A serial dilution of HIV-1 IIIB viruses

490   with known concentrations at a series of dilutions were used to create a standard curve for the

491   absolute quantification of reactivated HIV-1 viruses in supernatants.

492   **Statistics**

493   Statistical analysis was performed using GraphPad PRISM. Data are presented as mean ±

494   standard error of the mean (SEM) of biological repeats from at least 3 independent experiments. *

495   $p<0.05$, ** $p<0.01$, *** $p<0.001$, or **** $p<0.001$ indicated the significant difference analyzed by

496   ANOVA and Tukey's multiple comparison test.

497

498

23

Reference

1. Ruelas, D.S. and W.C. Greene, *An integrated overview of HIV-1 latency.* Cell, 2013. **155**(3): p. 519-29.

2. Archin, N.M., et al., *Administration of vorinostat disrupts HIV-1 latency in patients on antiretroviral therapy.* Nature, 2012. **487**(7408): p. 482-5.

3. Kim, J.T., et al., *Latency reversal plus natural killer cells diminish HIV reservoir in vivo.* Nat Commun, 2022. **13**(1): p. 121.

4. Garrido, C., et al., *Interleukin-15-Stimulated Natural Killer Cells Clear HIV-1-Infected Cells following Latency Reversal Ex Vivo.* J Virol, 2018. **92**(12).

5. Siliciano, J.D., et al., *Stability of the latent reservoir for HIV-1 in patients receiving valproic acid.* J Infect Dis, 2007. **195**(6): p. 833-6.

6. Shan, L., et al., *Stimulation of HIV-1-specific cytolytic T lymphocytes facilitates elimination of latent viral reservoir after virus reactivation.* Immunity, 2012. **36**(3): p. 491-501.

7. Huang, S.H., et al., *Latent HIV reservoirs exhibit inherent resistance to elimination by CD8+ T cells.* J Clin Invest, 2018. **128**(2): p. 876-889.

8. Clayton, K.L., et al., *Resistance of HIV-infected macrophages to CD8(+) T lymphocyte-mediated killing drives activation of the immune system.* Nat Immunol, 2018. **19**(5): p. 475-486.

9. Ren, Y., et al., *BCL-2 antagonism sensitizes cytotoxic T cell-resistant HIV reservoirs to elimination ex vivo.* J Clin Invest, 2020. **130**(5): p. 2542-2559.

10. Alter, G., et al., *HIV-1 adaptation to NK-cell-mediated immune pressure.* Nature, 2011. **476**(7358): p. 96-100.

11. Elemans, M., et al., *HIV-1 adaptation to NK cell-mediated immune pressure.* PLoS Pathog, 2017. **13**(6): p. e1006361.

12. Rahman, S.A., et al., *Lymph node CXCR5+ NK cells associate with control of chronic SHIV infection.* JCI Insight, 2022. **7**(8).

13. Luteijn, R., et al., *Early viral replication in lymph nodes provides HIV with a means by which to escape NK-cell-mediated control.* Eur J Immunol, 2011. **41**(9): p. 2729-40.

14. Fukazawa, Y., et al., *B cell follicle sanctuary permits persistent productive simian immunodeficiency virus infection in elite controllers.* Nat Med, 2015. **21**(2): p. 132-9.

15. Huot, N., et al., *Natural killer cells migrate into and control simian immunodeficiency virus replication in lymph node follicles in African green monkeys.* Nat Med, 2017. **23**(11): p. 1277-1286.

16. Macedo, A.B., et al., *The HIV Latency Reversal Agent HODHBt Enhances NK Cell Effector and Memory-Like Functions by Increasing Interleukin-15-Mediated STAT Activation.* J Virol, 2022: p. e0037222.

17. Huang, H., et al., *A CRISPR/Cas9 screen identifies the histone demethylase MINA53 as a novel HIV-1 latency-promoting gene (LPG).* Nucleic Acids Res, 2019. **47**(14): p. 7333-7347.

18. Mar, B.G., et al., *SETD2 alterations impair DNA damage recognition and lead to resistance to chemotherapy in leukemia.* Blood, 2017. **130**(24): p. 2631-2641.

19. Horton, J.R., et al., *Characterization of a Linked Jumonji Domain of the KDM5/JARID1 Family of Histone H3 Lysine 4 Demethylases.* J Biol Chem, 2016. **291**(6): p. 2631-46.

24

20. Xu, W., et al., *KDM5B demethylates H3K4 to recruit XRCC1 and promote chemoresistance.* Int J Biol Sci, 2018. **14**(9): p. 1122-1132.

21. Yoh, S.M., J.S. Lucas, and K.A. Jones, *The Iws1:Spt6:CTD complex controls cotranscriptional mRNA biosynthesis and HYPB/Setd2-mediated histone H3K36 methylation.* Genes Dev, 2008. **22**(24): p. 3422-34.

22. Vermeulen, M., et al., *Selective anchoring of TFIID to nucleosomes by trimethylation of histone H3 lysine 4.* Cell, 2007. **131**(1): p. 58-69.

23. Lauberth, S.M., et al., *H3K4me3 interactions with TAF3 regulate preinitiation complex assembly and selective gene activation.* Cell, 2013. **152**(5): p. 1021-36.

24. Collins, B.E., et al., *Histone H3 lysine K4 methylation and its role in learning and memory.* Epigenetics Chromatin, 2019. **12**(1): p. 7.

25. Barski, A., et al., *High-resolution profiling of histone methylations in the human genome.* Cell, 2007. **129**(4): p. 823-37.

26. Nguyen, K., et al., *Inhibition of the H3K27 demethylase UTX enhances the epigenetic silencing of HIV proviruses and induces HIV-1 DNA hypermethylation but fails to permanently block HIV reactivation.* PLoS Pathog, 2021. **17**(10): p. e1010014.

27. Zhang, H.S., et al., *UTX-1 regulates Tat-induced HIV-1 transactivation via changing the methylated status of histone H3.* Int J Biochem Cell Biol, 2016. **80**: p. 51-56.

28. Liu, Y., et al., *Lysine-specific demethylase 1 cooperates with BRAF-histone deacetylase complex 80 to enhance HIV-1 Tat-mediated transactivation.* Virus Genes, 2018. **54**(5): p. 662-671.

29. Petronikolou, N., J.E. Longbotham, and D.G. Fujimori, *Extended Recognition of the Histone H3 Tail by Histone Demethylase KDM5A.* Biochemistry, 2020. **59**(5): p. 647-651.

30. Plch, J., J. Hrabeta, and T. Eckschlager, *KDM5 demethylases and their role in cancer cell chemoresistance.* Int J Cancer, 2019. **144**(2): p. 221-231.

31. Secombe, J. and R.N. Eisenman, *The function and regulation of the JARID1 family of histone H3 lysine 4 demethylases: the Myc connection.* Cell Cycle, 2007. **6**(11): p. 1324-8.

32. Harmeyer, K.M., et al., *JARID1 Histone Demethylases: Emerging Targets in Cancer.* Trends Cancer, 2017. **3**(10): p. 713-725.

33. Wang, L., et al., *Enhancing KDM5A and TLR activity improves the response to immune checkpoint blockade.* Sci Transl Med, 2020. **12**(560).

34. Shi, L., et al., *LncRNA IFITM4P promotes immune escape by up-regulating PD-L1 via dual mechanism in oral carcinogenesis.* Mol Ther, 2022. **30**(4): p. 1564-1577.

35. Sperk, M., R.V. Domselaar, and U. Neogi, *Immune Checkpoints as the Immune System Regulators and Potential Biomarkers in HIV-1 Infection.* Int J Mol Sci, 2018. **19**(7).

36. Barber, D.L., et al., *Restoring function in exhausted CD8 T cells during chronic viral infection.* Nature, 2006. **439**(7077): p. 682-7.

37. Day, C.L., et al., *PD-1 expression on HIV-specific T cells is associated with T-cell exhaustion and disease progression.* Nature, 2006. **443**(7109): p. 350-4.

38. Banga, R., et al., *Lymph node migratory dendritic cells modulate HIV-1 transcription through PD-1 engagement.* PLoS Pathog, 2019. **15**(7): p. e1007918.

39. Munoz, O., et al., *Active PD-L1 incorporation within HIV virions functionally impairs T follicular helper cells.* PLoS Pathog, 2022. **18**(7): p. e1010673.

40. Wu, L., et al., *KDM5 histone demethylases repress immune response via suppression of STING.* PLoS Biol, 2018. **16**(8): p. e2006134.

41. Zhang, S.M., et al., *KDM5B promotes immune evasion by recruiting SETDB1 to silence retroelements.* Nature, 2021. **598**(7882): p. 682-687.

42. Parmar, N., P. Chandrakar, and S. Kar, *Leishmania donovani Subverts Host Immune Response by Epigenetic Reprogramming of Macrophage M(Lipopolysaccharides + IFN-gamma)/M(IL-10) Polarization.* J Immunol, 2020. **204**(10): p. 2762-2778.

43. Peng, D., et al., *Histone demethylase KDM5A promotes tumorigenesis of osteosarcoma tumor.* Cell Death Discov, 2021. **7**(1): p. 9.

44. Ohguchi, H., et al., *Lysine Demethylase 5A is Required for MYC Driven Transcription in Multiple Myeloma.* Blood Cancer Discov, 2021. **2**(4): p. 370-387.

45. Wei, X., et al., *Emergence of resistant human immunodeficiency virus type 1 in patients receiving fusion inhibitor (T-20) monotherapy.* Antimicrob Agents Chemother, 2002. **46**(6): p. 1896-905.

46. Sarzotti-Kelsoe, M., et al., *Optimization and validation of the TZM-bl assay for standardized assessments of neutralizing antibodies against HIV-1.* J Immunol Methods, 2014. **409**: p. 131-46.

47. Luo, Z., et al., *Differential Expression of CREM/ICER Isoforms Is Associated with the Spontaneous Control of HIV Infection.* mBio, 2022: p. e0197921.

48. Ptaschinski, C., et al., *RSV-Induced H3K4 Demethylase KDM5B Leads to Regulation of Dendritic Cell-Derived Innate Cytokines and Exacerbates Pathogenesis In Vivo.* PLoS Pathog, 2015. **11**(6): p. e1004978.

49. Herbeuval, J.P., et al., *Regulation of TNF-related apoptosis-inducing ligand on primary CD4+ T cells by HIV-1: role of type I IFN-producing plasmacytoid dendritic cells.* Proc Natl Acad Sci U S A, 2005. **102**(39): p. 13974-9.

50. Herbeuval, J.P., et al., *CD4+ T-cell death induced by infectious and noninfectious HIV-1: role of type 1 interferon-dependent, TRAIL/DR5-mediated apoptosis.* Blood, 2005. **106**(10): p. 3524-31.

51. Dagenais-Lussier, X., et al., *USP18 is a significant driver of memory CD4 T-cell reduced viability caused by type I IFN signaling during primary HIV-1 infection.* PLoS Pathog, 2019. **15**(10): p. e1008060.

52. Fraietta, J.A., et al., *Type I interferon upregulates Bak and contributes to T cell loss during human immunodeficiency virus (HIV) infection.* PLoS Pathog, 2013. **9**(10): p. e1003658.

53. Petrasek, J., et al., *STING-IRF3 pathway links endoplasmic reticulum stress with hepatocyte apoptosis in early alcoholic liver disease.* Proc Natl Acad Sci U S A, 2013. **110**(41): p. 16544-9.

54. Kutsch, O., et al., *Direct and quantitative single-cell analysis of human immunodeficiency virus type 1 reactivation from latency.* J Virol, 2002. **76**(17): p. 8776-86.

55. Duverger, A., et al., *Determinants of the establishment of human immunodeficiency virus type 1 latency.* J Virol, 2009. **83**(7): p. 3078-93.

56. Johansson, C., et al., *Structural analysis of human KDM5B guides histone demethylase inhibitor development.* Nat Chem Biol, 2016. **12**(7): p. 539-45.

57. Zhou, D., et al., *Inhibition of Polo-like kinase 1 (PLK1) facilitates the elimination of HIV-1 viral reservoirs in CD4(+) T cells ex vivo.* Sci Adv, 2020. **6**(29): p. eaba1941.

58. Lusic, M., et al., *Regulation of HIV-1 gene expression by histone acetylation and factor recruitment at the LTR promoter.* EMBO J, 2003. **22**(24): p. 6550-61.

59. Power, D., et al., *IFI44 suppresses HIV-1 LTR promoter activity and facilitates its latency.* Virology, 2015. **481**: p. 142-50.

60. Nixon, C.C., et al., *Systemic HIV and SIV latency reversal via non-canonical NF-kappaB signalling in vivo.* Nature, 2020. **578**(7793): p. 160-165.

61. Kolesnitchenko, V., et al., *A major human immunodeficiency virus type 1-initiated killing pathway distinct from apoptosis.* J Virol, 1997. **71**(12): p. 9753-63.

62. Chaitanya, G.V., A.J. Steven, and P.P. Babu, *PARP-1 cleavage fragments: signatures of cell-death proteases in neurodegeneration.* Cell Commun Signal, 2010. **8**: p. 31.

63. Alvarez-Carbonell, D., et al., *Toll-like receptor 3 activation selectively reverses HIV latency in microglial cells.* Retrovirology, 2017. **14**(1): p. 9.

64. Alvarez-Carbonell, D., et al., *The Glucocorticoid Receptor Is a Critical Regulator of HIV Latency in Human Microglial Cells.* J Neuroimmune Pharmacol, 2019. **14**(1): p. 94-109.

65. Alvarez-Carbonell, D., et al., *Cross-talk between microglia and neurons regulates HIV latency.* PLoS Pathog, 2019. **15**(12): p. e1008249.

66. Folks, T.M., et al., *Cytokine-induced expression of HIV-1 in a chronically infected promonocyte cell line.* Science, 1987. **238**(4828): p. 800-2.

67. Folks, T.M., et al., *Characterization of a promonocyte clone chronically infected with HIV and inducible by 13-phorbol-12-myristate acetate.* J Immunol, 1988. **140**(4): p. 1117-22.

68. Symons, J., et al., *HIV integration sites in latently infected cell lines: evidence of ongoing replication.* Retrovirology, 2017. **14**(1): p. 2.

69. Archin, N.M., et al., *Valproic acid without intensified antiviral therapy has limited impact on persistent HIV infection of resting CD4+ T cells.* AIDS, 2008. **22**(10): p. 1131-5.

70. Lehrman, G., et al., *Depletion of latent HIV-1 infection in vivo: a proof-of-concept study.* Lancet, 2005. **366**(9485): p. 549-55.

71. Archin, N.M., et al., *Expression of latent HIV induced by the potent HDAC inhibitor suberoylanilide hydroxamic acid.* AIDS Res Hum Retroviruses, 2009. **25**(2): p. 207-12.

72. Contreras, X., et al., *Suberoylanilide hydroxamic acid reactivates HIV from latently infected cells.* J Biol Chem, 2009. **284**(11): p. 6782-9.

73. Edelstein, L.C., et al., *Short communication: activation of latent HIV type 1 gene expression by suberoylanilide hydroxamic acid (SAHA), an HDAC inhibitor approved for use to treat cutaneous T cell lymphoma.* AIDS Res Hum Retroviruses, 2009. **25**(9): p. 883-7.

74. Sagot-Lerolle, N., et al., *Prolonged valproic acid treatment does not reduce the size of latent HIV reservoir.* AIDS, 2008. **22**(10): p. 1125-9.

75. Archin, N.M., et al., *Antiretroviral intensification and valproic acid lack sustained effect on residual HIV-1 viremia or resting CD4+ cell infection.* PLoS One, 2010. **5**(2): p. e9390.

76. Archin, N.M., et al., *HIV-1 expression within resting CD4+ T cells after multiple doses of vorinostat.* J Infect Dis, 2014. **210**(5): p. 728-35.

77. Fidler, S., et al., *Antiretroviral therapy alone versus antiretroviral therapy with a kick and kill approach, on measures of the HIV reservoir in participants with recent HIV*

687   *infection (the RIVER trial): a phase 2, randomised trial.* Lancet, 2020. **395**(10227): p.
688   888-898.

689 78.   Elliott, J.H., et al., *Activation of HIV transcription with short-course vorinostat in HIV-*
690   *infected patients on suppressive antiretroviral therapy.* PLoS Pathog, 2014. **10**(10): p.
691   e1004473.

692 79.   Rasmussen, T.A., et al., *Panobinostat, a histone deacetylase inhibitor, for latent-virus*
693   *reactivation in HIV-infected patients on suppressive antiretroviral therapy: a phase 1/2,*
694   *single group, clinical trial.* Lancet HIV, 2014. **1**(1): p. e13-21.

695 80.   Archin, N.M., et al., *Interval dosing with the HDAC inhibitor vorinostat effectively*
696   *reverses HIV latency.* J Clin Invest, 2017. **127**(8): p. 3126-3135.

697 81.   Margolis, D.M., *Histone deacetylase inhibitors and HIV latency.* Curr Opin HIV AIDS,
698   2011. **6**(1): p. 25-9.

699 82.   Klein, B.J., et al., *The histone-H3K4-specific demethylase KDM5B binds to its substrate*
700   *and product through distinct PHD fingers.* Cell Rep, 2014. **6**(2): p. 325-35.

701 83.   Li, Q., et al., *Binding of the JmjC demethylase JARID1B to LSD1/NuRD suppresses*
702   *angiogenesis and metastasis in breast cancer cells by repressing chemokine CCL14.*
703   Cancer Res, 2011. **71**(21): p. 6899-908.

704 84.   Nishibuchi, G., et al., *Physical and functional interactions between the histone H3K4*
705   *demethylase KDM5A and the nucleosome remodeling and deacetylase (NuRD) complex.*
706   J Biol Chem, 2014. **289**(42): p. 28956-70.

707 85.   Ren, Z., et al., *A PRC2-Kdm5b axis sustains tumorigenicity of acute myeloid leukemia.*
708   Proc Natl Acad Sci U S A, 2022. **119**(9).

709 86.   Hasselgren, P.O., *Ubiquitination, phosphorylation, and acetylation--triple threat in*
710   *muscle wasting.* J Cell Physiol, 2007. **213**(3): p. 679-89.

711 87.   Zierhut, C., et al., *The Cytoplasmic DNA Sensor cGAS Promotes Mitotic Cell Death.*
712   Cell, 2019. **178**(2): p. 302-315 e23.

713 88.   Quillay, H., et al., *NK cells control HIV-1 infection of macrophages through soluble*
714   *factors and cellular contacts in the human decidua.* Retrovirology, 2016. **13**(1): p. 39.

715 89.   Yang, Y., et al., *MicroRNA let-7i Inhibits Histone Lysine Demethylase KDM5B to Halt*
716   *Esophageal Cancer Progression.* Mol Ther Nucleic Acids, 2020. **22**: p. 846-861.

717 90.   Wang, X., et al., *Overcoming radio-resistance in esophageal squamous cell carcinoma*
718   *via hypermethylation of PIK3C3 promoter region mediated by KDM5B loss.* J Radiat
719   Res, 2022. **63**(3): p. 331-341.

720 91.   Hennessy, E.J., et al., *Discovery of a novel class of dimeric Smac mimetics as potent IAP*
721   *antagonists resulting in a clinical candidate for the treatment of cancer (AZD5582).* J
722   Med Chem, 2013. **56**(24): p. 9897-919.

723 92.   Sun, S.C., *The non-canonical NF-kappaB pathway in immunity and inflammation.* Nat
724   Rev Immunol, 2017. **17**(9): p. 545-558.

725 93.   Zhuang, J., et al., *Selective IAP inhibition results in sensitization of unstimulated but not*
726   *CD40-stimulated chronic lymphocytic leukaemia cells to TRAIL-induced apoptosis.*
727   Pharmacol Res Perspect, 2014. **2**(6): p. e00081.

728 94.   Polanski, R., et al., *Caspase-8 activation by TRAIL monotherapy predicts responses to*
729   *IAPi and TRAIL combination treatment in breast cancer cell lines.* Cell Death Dis, 2015.
730   **6**: p. e1893.

95. Campbell, G.R., et al., *SMAC Mimetics Induce Autophagy-Dependent Apoptosis of HIV-1-Infected Resting Memory CD4+ T Cells.* Cell Host Microbe, 2018. **24**(5): p. 689-702 e7.

96. Hattori, S.I., et al., *Combination of a Latency-Reversing Agent With a Smac Mimetic Minimizes Secondary HIV-1 Infection in vitro.* Front Microbiol, 2018. **9**: p. 2022.

97. Sreeram, S., et al., *The potential role of HIV-1 latency in promoting neuroinflammation and HIV-1-associated neurocognitive disorder.* Trends Immunol, 2022. **43**(8): p. 630-639.

98. Zhu, J., et al., *Reactivation of latent HIV-1 by inhibition of BRD4.* Cell Rep, 2012. **2**(4): p. 807-16.

99. Kong, W., et al., *Nucleolar protein NOP2/NSUN1 suppresses HIV-1 transcription and promotes viral latency by competing with Tat for TAR binding and methylation.* PLoS Pathog, 2020. **16**(3): p. e1008430.

100. Jean, M.J., et al., *Curaxin CBL0100 Blocks HIV-1 Replication and Reactivation through Inhibition of Viral Transcriptional Elongation.* Front Microbiol, 2017. **8**: p. 2007.

101. Huang, F., et al., *Inosine Monophosphate Dehydrogenase Dependence in a Subset of Small Cell Lung Cancers.* Cell Metab, 2018. **28**(3): p. 369-382 e5.

102. Bosque, A. and V. Planelles, *Induction of HIV-1 latency and reactivation in primary memory CD4+ T cells.* Blood, 2009. **113**(1): p. 58-65.

103. Mousseau, G., et al., *The Tat Inhibitor Didehydro-Cortistatin A Prevents HIV-1 Reactivation from Latency.* mBio, 2015. **6**(4): p. e00465.

104. Huang, H., et al., *A Novel Bromodomain Inhibitor Reverses HIV-1 Latency through Specific Binding with BRD4 to Promote Tat and P-TEFb Association.* Front Microbiol, 2017. **8**: p. 1035.
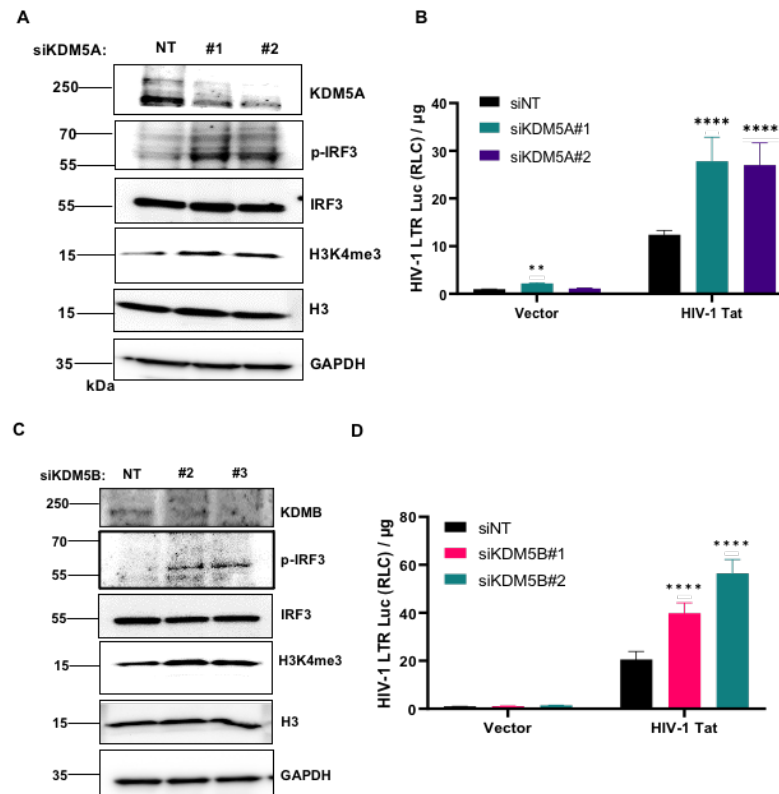
Fig 1 siRNA Knockdown of KDM5A/B increases the HIV-1 Tat/LTR-driven transcription. TZM-bl cells were received from reverse transfection by KDM5A siRNA # 1-2 or KDM5B siRNA #1-2 for 48h, and cells were trypsinized and reverse transfected by pQC empty vector or pQC-HIV-1 Tat for 48h. (**A**) KDM5A siRNA KD cells were harvested and lysed for IB of anti-KDM5A, p-IRF3/IRF3, GAPDH, and H3K4me3/H3. (**B**) KDM5A siRNA KD Cells with or without HIV-1 Tat overexpression were harvested for luciferase reporter assay. (**C**) KDM5B siRNA KD cells were harvested and lysed for IB of anti-KDM5B, p-IRF3/IRF, GAPDH, and H3K4me3/H3. (**D**) KDM5B siRNA KD cells with or without HIV-1 Tat overexpression were harvested for luciferase reporter assay. The readouts of RLU/total protein input (μg) were normalized with the siNT/pQC-empty vector-transfected TZM-bl control group. Results were calculated from at least 3 independent experiments and presented as mean +/- standard error of the mean (SEM). (** $p < 0.01$; **** $p < 0.0001$ by two-way ANOVA and Tukey's multiple comparison test compared to the same treated siNT control).
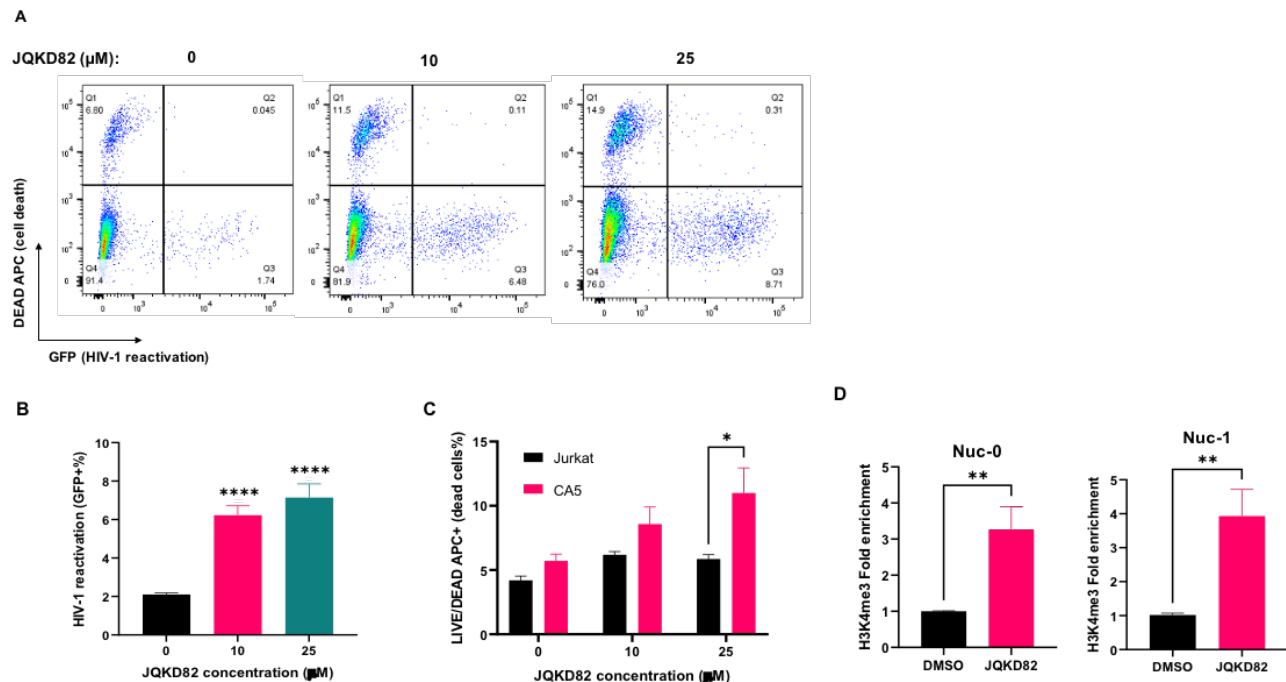
**Fig 2 KDM5 inhibitor JQKD82 induces the HIV-1 reactivation, cell death, and H3K4me3 at HIV-1 LTR in the latent infected CA5 cells.** (**A**) CA5 cells were treated with 0, 10, or 25 µM JQKD82 for 5 days. Cells were harvested for LIVE/DEAD staining and analyzed with FASC to identify the expression of HIV-1 LTR-driven GFP (**B**) and LIVE/DEAD-APC (**C**). CA5 cells were treated with DMSO or 25 µM JQKD82 for 5 days and then harvested to perform the ChIP qPCR assay of H3K4me3 (**D**) focusing on HIV-1 LTR Nuc-0 and Nuc-1 sites. Results were calculated from at least 3 independent experiments and presented as mean +/- standard error of the mean (SEM). (*$p < 0.05$; ** $p < 0.01$; **** $p < 0.0001$ by one-way/two-way ANOVA and Tukey's multiple comparison test compared to untreated (**B, D**) or parental cells control group (**C**)).
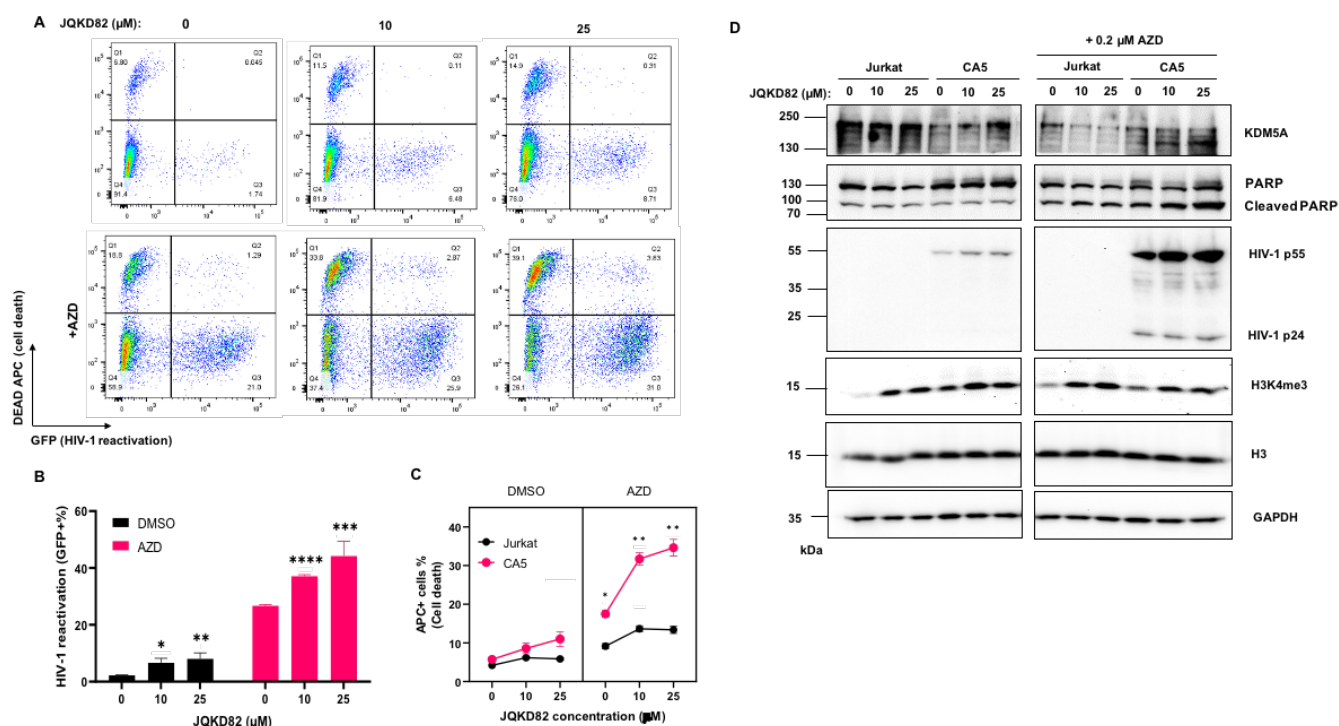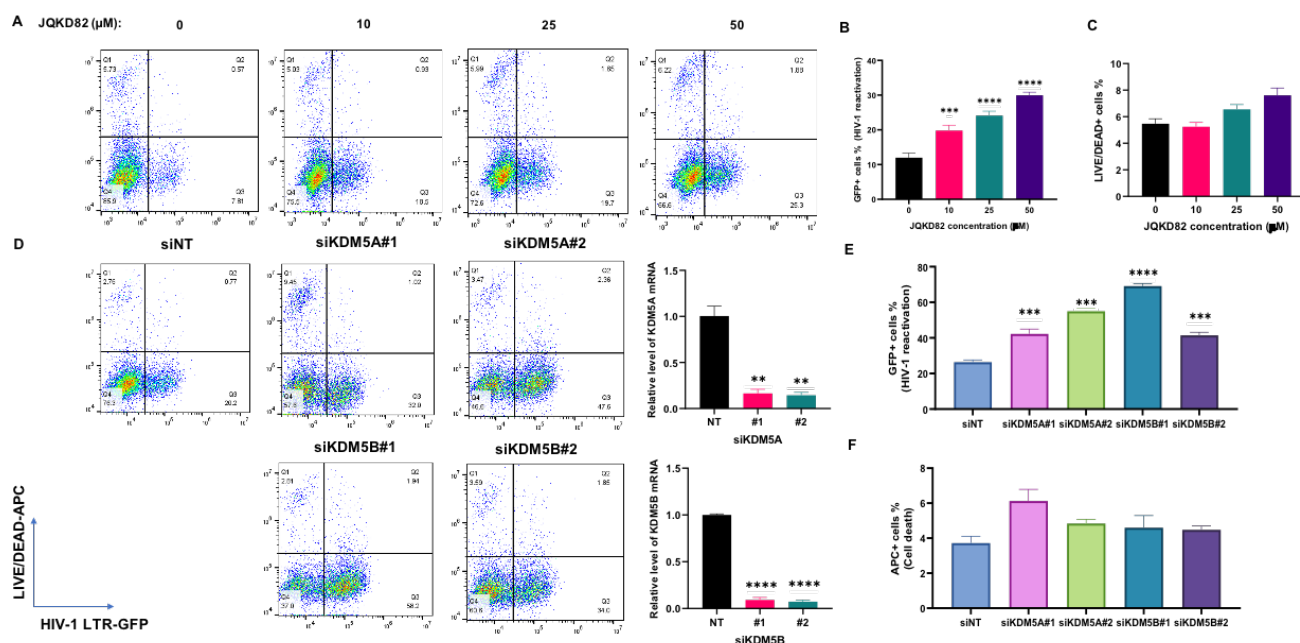
Fig 3 JQKD82/AZD5582 combination treatment synergistically increases the HIV-1 reactivation and cell death in CA5 cells. (**A**) CA5 cells were treated with 0, 10, or 25 μM JQKD82 for 3 days and refreshed the JQKD82-treated medium with or without 0.2 μM AZD5582 for 48h. Cells were performed the LIVE/DEAD staining and analyzed by FASC. (**B**) Treated CA5 cells were analyzed by the GFP expression from the HIV-1 reactivation. Results were calculated from 3 independent experiments and were presented as mean +/- standard error of the mean (SEM). (*p <0.05; ** p <0.01; *** p < 0.001; **** p <0.0001 by 2-way ANOVA and Tukey's multiple comparison test compared to 0 μM JQKD82-treated control). (**C**) Treated CA5 and parental Jurkat cells were analyzed for the LIVE/DEAD APC expression. Results were calculated from 3 independent experiments and were presented as mean +/- standard error of the mean (SEM). (*p <0.05; ** p <0.01 by 3-way ANOVA and Tukey's multiple comparison test compared to Jurkat cells under the same treatment.). (**D**) Jurkat and CA5 cells were treated with JQKD82/AZD and harvested for immunoblotting.
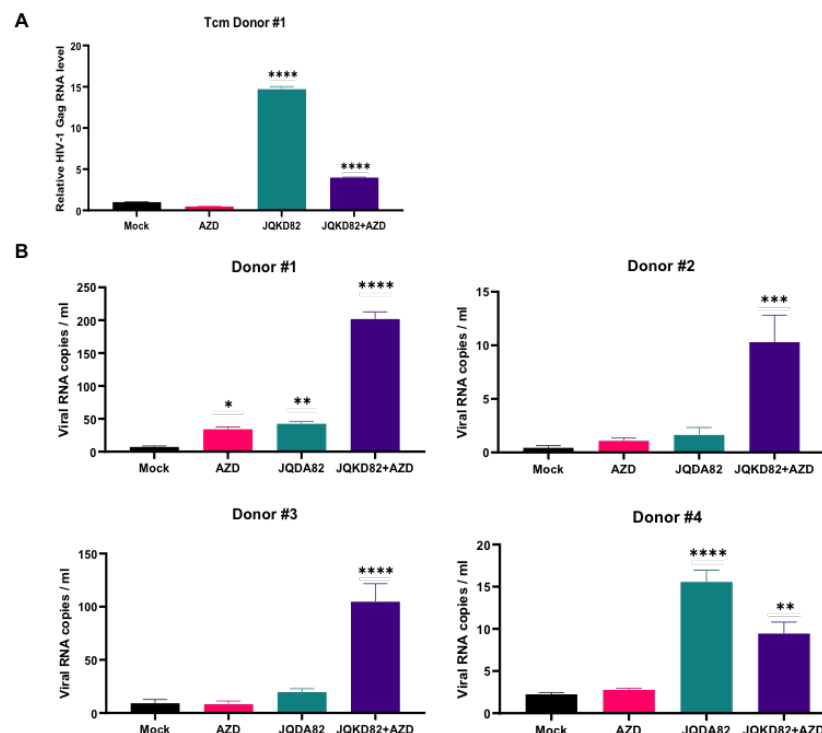
Fig 4 JQKD82/AZD5582 combinatory treatment induced HIV-1 reactivation in the primary T cells and HIV-1 patients' PBMCs. (**A**) The primary Tcm latency model was established by DHIV-1 infection. The DHIV-1 infected Tcm cells were back to latency and treated with DMSO or 10 µM JQKD82 for 3 days and then refreshed the treated medium for JQKD82-treated medium for an additional 3 days with or without 0.1 µM AZD5582. Cells were harvested for RNA extraction and RT-qPCR analysis for HIV-1 Gag mRNA level. (**B**) The HIV-1 patients' PBMC with CD8$^+$ T cell-depletion for Donor #1-4 and treated with DMSO or 10 µM JQKD82 for 3 days. Then these cells were refreshed with the JQKD82-treated medium for an additional 3 days with or without 0.1 µM AZD5582. Cultured supernatant was harvested for viral RNA extraction and ultrasensitive nested RT-qPCR analysis and normalized the viral RNA copies with HIV-1 III titration standard curve. Results were calculated from 3 technical repeats and presented as mean +/- standard error of the mean (SEM). (* $p<0.05$, ** $p<0.01$; **** $p<0.0001$ by one-way ANOVA and Tukey's multiple comparison test compared higher to mock control group).

bioRxiv preprint doi: https://doi.org/10.1101/2022.11.17.516956; this version posted November 17, 2022. The copyright holder for this preprint (which was not certified by peer review) is the author/funder, who has granted bioRxiv a license to display the preprint in perpetuity. It is made available under aCC-BY-NC 4.0 International license.

Fig 5 KDM5 inhibitor JQKD82 or siRNA knockdown of KDM5A/B induced the HIV-1 latency reactivation in HC69 microglia cells. (**A**) HC69 microglial cells were treated with 0, 10, 25, or 50 μM JQKD82 for 5 days. Cells were harvested for LIVE/DEAD staining and analyzed with FASC to identify the expression of HIV-1 LTR-driven GFP (**B**) and LIVE/DEAD-APC (**C**). HC69 microglia cells were received from reverse transfection by KDM5A siRNA # 1-2, or KDM5B siRNA #1-2 for 72hr. The siRNA-transfected cells were harvested for RNA extraction and RT-qPCR to identify the siRNA KD efficiency. Cells were harvested for LIVE/DEAD staining and analyzed with FASC to identify the expression of HIV-1 LTR-driven GFP (**E**) and cell death (**F**). Results were calculated from 3 independent experiments and presented as mean +/- standard error of the mean (SEM). (*** p <0.001; **** p <0.0001 by one-way ANOVA and Tukey's multiple comparison test compared to the untreated or SiNT control group).
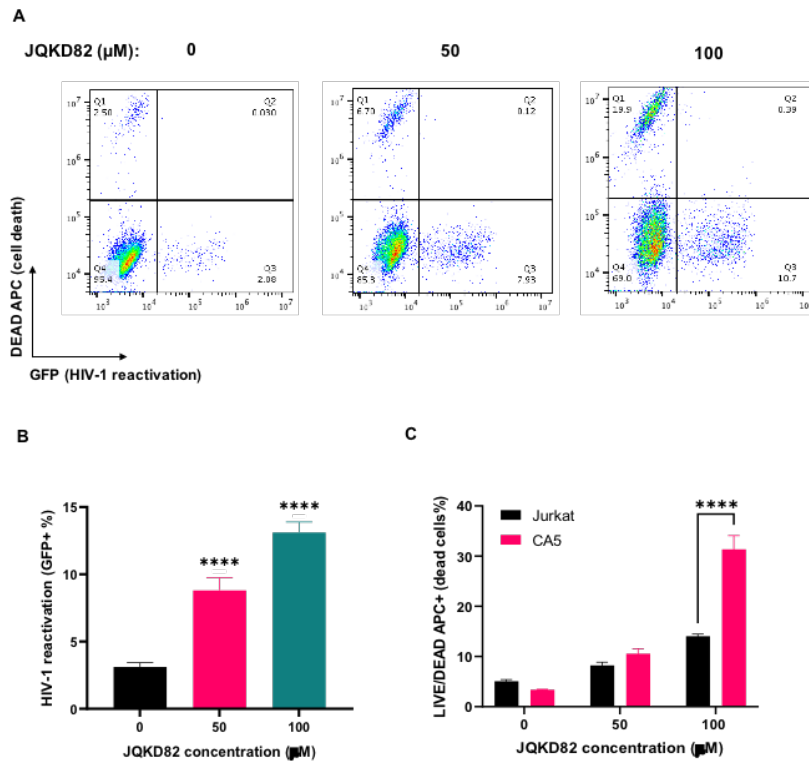
Fig S1 Short-time treatment of JQKD82 in CA5 cells for HIV-1 reactivation and cell killing. CA5 cells were treated with 0, 50, or 100 µM JQKD82 for 48 h. Cells were harvested for LIVE/DEAD staining and analyzed with FASC to identify the expression of HIV-1 LTR-driven GFP (**A, B**) and LIVE/DEAD-APC (**C**). Results were calculated from at least 3 independent experiments and presented as mean +/- standard error of the mean (SEM). (** p <0.01; **** p <0.0001 by one-way/two-way ANOVA and Tukey's multiple comparison test compared to the untreated (**B**) or parental cell control group (**C**)).
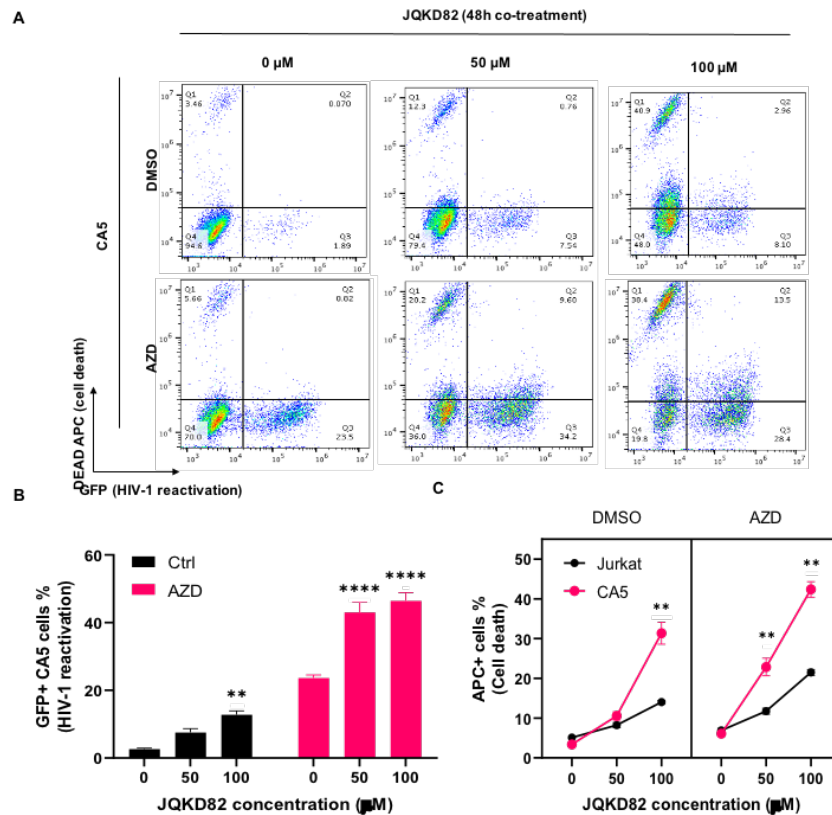
Fig S2 Short-time treatment of JQKD82/AZD5582 in CA5 cells for HIV-1 reactivation and cell killing. (**A**) CA5 cells were treated with 0, 50, or 100 μM with or without 0.2 μM AZD5582 for 48h. Cells were performed the LIVE/DEAD staining and analyzed by FASC. (**B**) Treated CA5 cells were analyzed by the GFP expression from the HIV-1 reactivation. Results were calculated from 3 independent experiments and were presented as mean +/- standard error of the mean (SEM). (** $p < 0.01$; **** $p < 0.0001$ by 2-way ANOVA and Tukey's multiple comparison test compared to 0 μM JQKD82 treated group). (**C**) Treated CA5 cells were analyzed for the LIVE/DEAD APC expression. Results were calculated from 3 independent experiments and were presented as mean +/- standard deviation (SEM). (**$p < 0.01$ by 3-way ANOVA and Tukey's multiple comparison test compared to Jurkat cells under the same treatment.).
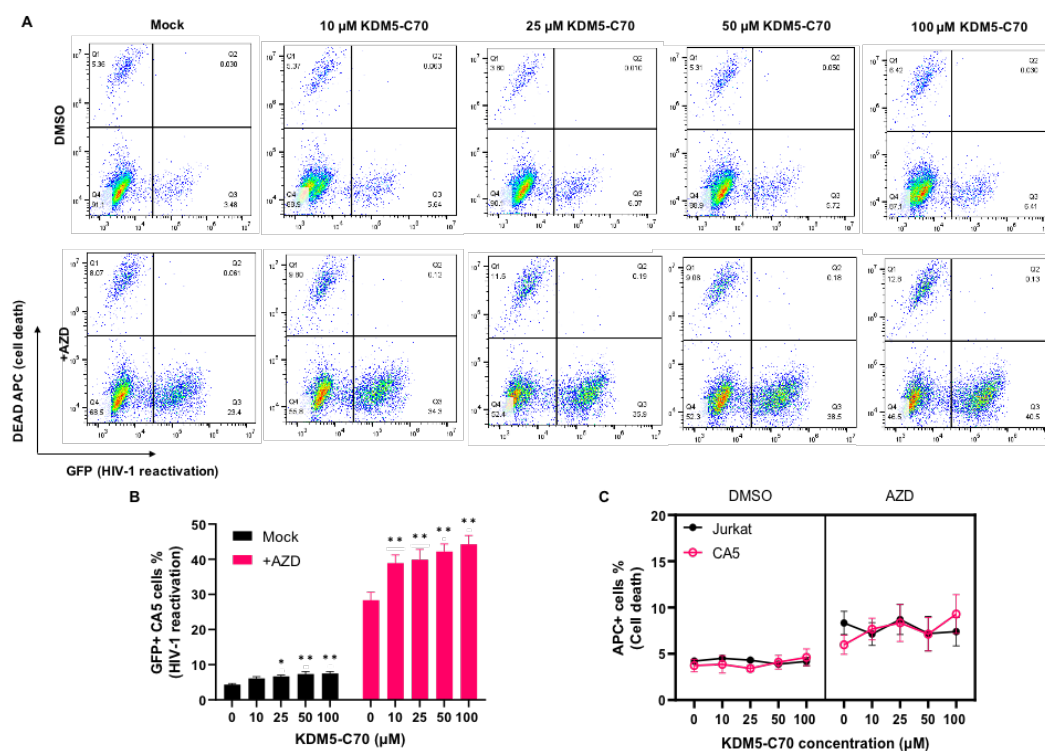
Fig S3 KDM5 inhibitor KDM5-C70 increased the HIV-1 reactivation in CA5 cells. (**A**) CA5 cells were treated with 0, 10, 25, 50, or 100 µM KDM5C-70 with or without 0.2 µM AZD5582 for 48h. Cells were performed the LIVE/DEAD staining and analyzed by FASC. (**B**) Treated CA5 cells were analyzed by the GFP expression from the HIV-1 reactivation. Results were calculated from 2 independent experiments and were presented as mean +/- standard error of the mean. (* $p < 0.05$; ** $p < 0.01$ by 2-way ANOVA and Tukey's multiple comparison test compared to 0 µM KDM5-C70 treated group). (**C**) Treated CA5 and Jurkat parental cells were analyzed for the LIVE/DEAD APC expression. Results were calculated from 2 independent experiments and were presented as mean +/- standard error of the mean (SEM).
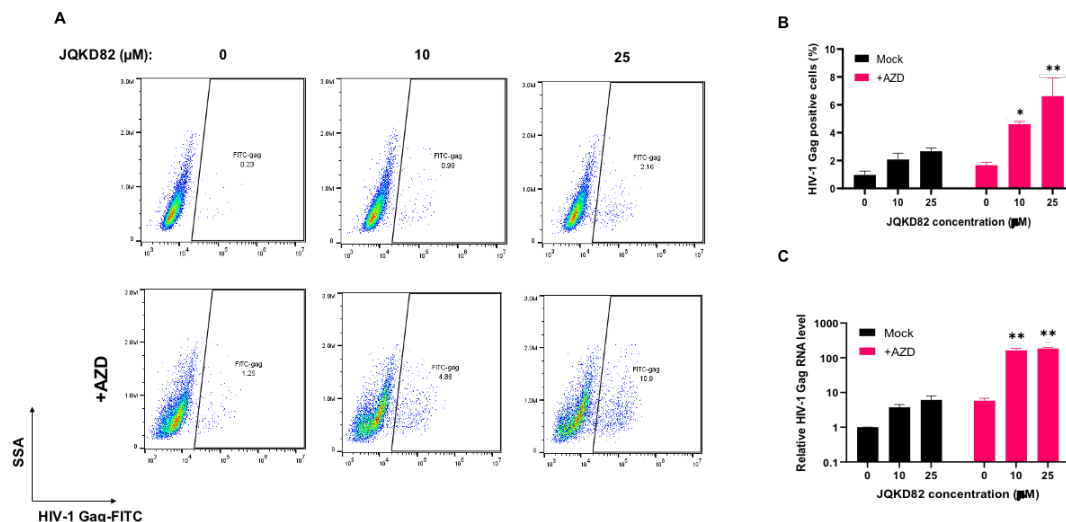
Fig S4 JQKD82/AZD5582 combinatory treatment increases the HIV-1 reactivation in U1/HIV monocyte cell line. (**A**) U1/HIV cells were treated with 0, 10, or 25 µM JQKD82 for 3 days and refreshed the treated medium with or without 0.2 µM AZD5582 for 48h. Cells were performed anti-HIV-1 Gag intracellular staining (**B**). Treated cells were harvested for RNA extraction and RT-qPCR to detect the HIV-1 Gag mRNA level (**C**). Results were calculated from at least 2 independent experiments and presented as mean +/- standard deviation (SD). (* p <0.05; ** p < 0.01; by two-way ANOVA and Tukey's multiple comparison test compared to 0 µM JQKD82-treated control.)